INTERNATIONAL JOURNAL FOR NUMERICAL METHODS IN FLUIDS, VOL. 4, 711–724 (1984)

NUMERICAL PREDICTIONS OF FLOWS OVER BACKWARD-FACING STEPS

L. P. HACKMAN,* G. D. RAITHBY AND A. B. STRONG

Department of Mechanical Engineering, University of Waterloo, Waterloo, Ontario, Canada N2L 3G1

SUMMARY

Predictions are reported for two-dimensional, steady, incompressible flows over rearward-facing steps for both laminar and turbulent conditions. The standard k–ε turbulence model was used for the turbulent flow. Attention was focused on obtaining accurate solutions to the differential equations. It is concluded that some of the serious discrepancies that have occurred between prediction and observation, and attributed in earlier studies to the inadequacy of the turbulence model, may have been due to the inaccuracy of the solution.

KEY WORDS Finite-Volume Method Numerical Diffusion Upstream Weighted Differencing Skew Upstream Differencing Turbulent Recirculating Flow Turbulence Model

INTRODUCTION

Many of the fluid flows of practical interest are turbulent and have one or more recirculation zones. To improve the performance of aerofoils or rotating machinery designs, modifications are made to reduce or eliminate recirculation zones. In other cases, such as flow in a combustor, recirculation is a prerequisite for successful operation. Numerical models that are capable of accurately simulating such flows are desirable as one means of economically improving designs.

Such numerical models consist of a mathematical model and a solution algorithm. The 'mathematical model' is defined here as the set of differential equations, algebraic relations and boundary conditions, which include the mass and mean momentum equations, the turbulence model for the estimation of mean turbulence exchange, etc., whose solution is sought. These equations, particularly the turbulence model, embody approximations so that the accuracy of the mathematical model needs to be verified by a comparison with measurements for the types of problems of interest. The solution algorithm, typically a finite volume or finite element method, does not yield an exact solution to the mathematical model. The final predictions therefore contain errors from two independent sources. To draw a definitive conclusion about the mathematical model itself, the solution to the equations and the experimental data should both be sufficiently accurate that serious differences between prediction and observation can be confidently attributed to the failure of the mathematical model. The authors are not aware of any studies involving turbulent recirculating flows where these conditions were unequivocally satisfied. The current trend of attributing poor

* Current address: Research Engineer, Syncrude Canada Ltd. (Research), P.O. Box 5790, Edmonton, Alberta, Canada T6C 4G3

0271-2091/84/080711-14$01.40

Received 8 February 1983
Revised 22 July 1983

predictions for such flows to the inadequacy of the turbulence model is therefore, at best, premature and, at worst, incorrect. It was the goal of the present study to obtain sufficiently accurate solutions to one complex flow problem that the performance of the standard k–ε turbulence model[1] could be evaluated confidently.

The criteria for choosing the problem were that the flow must be steady, two-dimensional, recirculating and turbulent, and that accurate data must be available. The 'two-dimensional' flow over a backward-facing step, with the data by Kim,[2] appeared to satisfy these criteria most closely. The present paper therefore reports predictions for this flow.

An extensive review of the literature which relates to the prediction of complex turbulent flows has been reported by Hackman,[3] and only a few of the particularly relevant studies are mentioned here. The fact that numerical errors can severely distort the predictions from turbulence models was pointed out by Militzer *et al.*,[4] with more detailed studies by Leschziner and Rodi.[5] The inadequacy of upstream differencing schemes for flows over a step and a fence were clearly pointed out by Castro.[6] McGuirk *et al.*[7] proposed a method of identifying regions within the flow where numerical diffusion errors are important, and Castro *et al.*[8] pointed out the deficiencies of upwind differencing for laminar flow normal to a flat plate. Other recent predictions of flow over fences and steps have been carried out by Kim,[2] Kwon and Pletcher[9] and Durst and Rastogi.[10] Launder[11] compared the predictions of flow over a backward-facing step with the data of Kim, and concluded that the k–ε turbulence model has serious deficiencies for this flow; the possible contamination of the predictions by numerical error was not fully addressed.

The literature review reveals that there are often substantial discrepancies between predictions and measurement for turbulent recirculating flows, but it is not usually clear whether these stem from a poor turbulence model, an inaccurate solution, or inaccurate experimental data. This paper will attempt to obtain sufficiently accurate solutions to the backward-facing step problem that the performance of the k–ε turbulence model can be evaluated with an added degree of confidence.

FORMULATION AND SOLUTION METHOD

Geometry

The flow configuration of interest in this study is depicted in Figure 1. Fluid enters from the left through a parallel plate channel of depth H, flows over a step of height h, and leaves

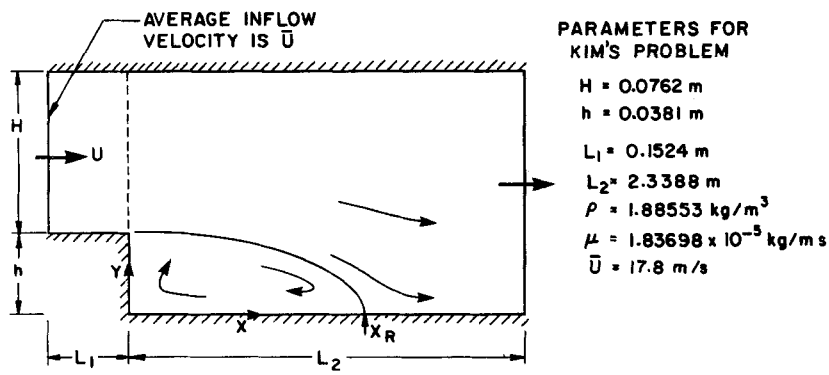

Figure 1. Definition sketch for flow over a backward-facing step. The geometry and fluid properties for Kim's turbulent flow problem 2 are defined at the right-hand side of the figure

at the right through a channel of depth $h+H$. The average inflow velocity is $\bar{U}$. For sufficiently high Reynolds numbers the flow is known to detach at the corner and reattach on the lower wall at some distance X_R downstream. The motion is assumed to be steady, two-dimensional and incompressible.

The mathematical model

The equations embodying the mathematical model can be written in any of several co-ordinate systems. The exact solution to the equation set must be independent of the co-ordinate system used, but the errors that arise in the numerical solution will be different for different systems. In the present study the problem was solved using two different co-ordinate systems; a comparison of these results provides one indicator of the solution accuracy. Both co-ordinate systems were orthogonal and isometric (i.e. the metrics in both co-ordinate directions were equal).

The details of the derivation of the conservation equations and the k–ε turbulence model in general orthogonal curvilinear co-ordinates may be found in the thesis of Hackman.[3] The equations are summarized in Table I, wherein x and y are the general orthogonal co-ordinates and h is the local metric. The time mean velocities in the x- and y-directions are U and V, respectively, k and ε are the turbulent kinetic energy and its dissipation,[1] and P^* is the local effective pressure in the mean-flow momentum equations. Fluid properties have been taken as uniform. With some manipulation, this equation set can be shown to be identical to that used by Pope.[12] The constants in the k–ε model are those proposed by Launder and Spalding.[1]

The numerical model

Grid. The equations in Table I were solved over the region downstream of the step using a Cartesian system, as shown in Figure 2(a), and the boundary-fitted isometric orthogonal curvilinear system illustrated in Figure 2(b). The latter was derived using a Schwarz–Christoffel transformation.[13] A series of numerical experiments established that the predicted flow field was particularly sensitive to the grid spacing near the step in the main flow direction, and to the cross-flow spacing in the shear layer just downstream from the lip of the step. Selective grid refinement was used to pack the grid in these regions. Numerical experiments also revealed that the predicted flow in the recirculation zone was independent of the location of the downstream boundary, provided that it was placed at least $3h$ beyond the reattachment point. The reported calculations were all made with downstream boundaries located at least $7h$ beyond reattachment.

Finite-volume equations. A finite volume method[14] was used to formulate the algebraic-equation approximations to the differential equations. This involved first integrating the differential equations over control volumes defined by the grid. A staggered grid was used[14] whereby the control volumes for U and V were centred on the faces of the control volume for continuity, k and ε; pressure nodes were located at the centre of the continuity control volume. The integral equations were reduced to algebraic equations using two different sets of approximations. The schemes that resulted are denoted as UWDS and SHUDS.

In the first of these, the Upstream Weighted Differencing Scheme (UWDS) of Raithby and Torrance[15] was used. This is derived by approximating the fluxes by convection and diffusion across control-volume faces using a one-dimensional solution to the differential equations between the grid points on either side of the face. The exponentials that arise are

Table I. Governing equations written in two dimensional isometric orthogonal curvilinear co-ordinates

The general equation is of the form

$$\frac{\partial}{\partial t}(\rho\phi)+\nabla(1)\left[\rho U\phi-\Gamma\frac{1}{h}\frac{\partial\phi}{\partial x}\right]+\nabla(2)\left[\rho V\phi-\Gamma\frac{1}{h}\frac{\partial\phi}{\partial y}\right]=\dot{S}_\phi$$

where

$$\nabla(1)[\ ]=\frac{1}{hh}\frac{\partial}{\partial x}(h[\ ]) \quad \text{and} \quad \nabla(2)[\ ]=\frac{1}{hh}\frac{\partial}{\partial y}(h[\ ])$$

ϕ	Γ	$\dot{S}_\phi$
1	0	0
U	μ_{eff}	$-\frac{1}{h}\frac{\partial P^*}{\partial x}+\nabla(1)\left[\mu_{eff}\left(\tau(11)-\frac{1}{h}\frac{\partial U}{\partial x}\right)\right]+\nabla(2)\left[\mu_{eff}\left(\tau(21)-\frac{1}{h}\frac{\partial U}{\partial y}\right)\right]$ $+H(1)[\rho VV-\mu_{eff}\tau(22)]-H(2)[\rho UV-\mu_{eff}\tau(21)]$
V	μ_{eff}	$-\frac{1}{h}\frac{\partial P^*}{\partial y}+\nabla(1)\left[\mu_{eff}(\tau(12)-\frac{1}{h}\frac{\partial V}{\partial x})\right]+\nabla(2)\left[\mu_{eff}\left(\tau(22)-\frac{1}{h}\frac{\partial V}{\partial y}\right)\right]$ $+H(2)[\rho UU-\mu_{eff}\tau(11)]-H(1)[\rho UV-\mu_{eff}\tau(21)]$
k	$\frac{\mu_t}{\sigma_k}+\mu$	$P_k-\rho\varepsilon$
ε	$\frac{\mu_t}{\sigma_\varepsilon}+\mu$	$\frac{\varepsilon}{k}(C_1P_k-C_2\rho\varepsilon)$

where

$$H(1)=-\frac{1}{hh}\frac{\partial h}{\partial x}$$

$$H(2)=\frac{1}{hh}\frac{\partial h}{\partial y}$$

$$\tau(11)=2\left[\frac{1}{h}\frac{\partial U}{\partial x}+VH(2)\right]$$

$$\tau(12)=\left[\frac{1}{h}\frac{\partial U}{\partial y}-VH(1)+\frac{1}{h}\frac{\partial V}{\partial x}-UH(1)\right]=\tau(21)$$

$$\tau(22)=2\left[\frac{1}{h}\frac{\partial V}{\partial y}+UH(1)\right]$$

$$P_k=\frac{1}{2}\mu_t[\tau(11)^2+2\tau(12)^2+\tau(22)^2]$$

$$P^*=\bar{P}+\frac{2}{3}\rho k$$

$$\mu_t=C_\mu\rho k^2/\varepsilon$$

$$C_\mu=0{\cdot}09$$

$$C_1=1{\cdot}92$$

$$C_2=1{\cdot}44$$

$$\sigma_\kappa=1{\cdot}0$$

$$\sigma_\varepsilon=1{\cdot}3$$

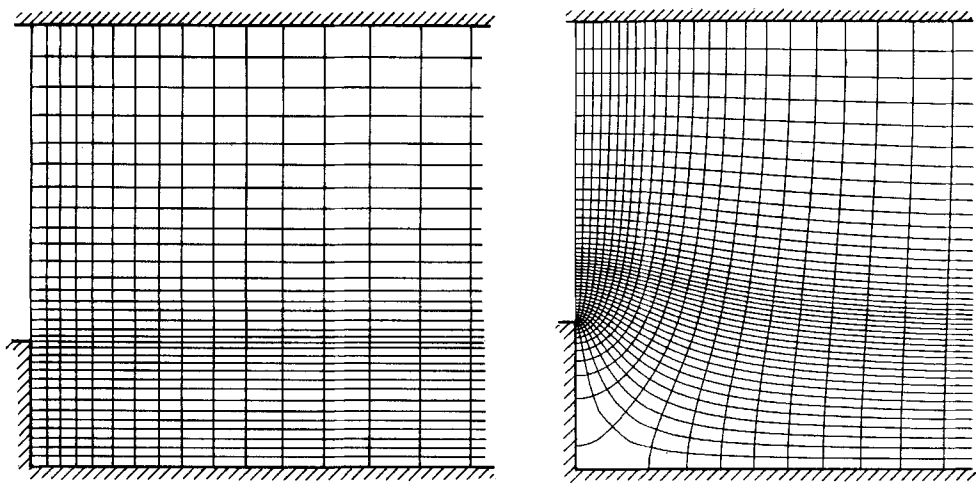

Figure 2. Typical grid distribution near the step for the Cartesian mesh (a), and curvilinear mesh (b). The complete mesh extended to 20 step heights downstream of the step face for all predictions reported in this paper

approximated in this scheme by simple algebraic functions. This scheme is very similar to the hybrid schemes of Patankar and Spalding;[16] all such schemes are known to suffer from the effects of 'false diffusion'.

More accurate solutions for a given grid can be obtained by improving the approximation of the convection fluxes crossing control volume faces. In the present study, a Skew Hybrid Upstream Differencing Scheme (SHUDS) was employed. The scheme was formulated such that for grid Peclet numbers at a control volume face in the range $Pe_\Delta \leq 1$, a full central difference is used; for $Pe_\Delta \geq 2$ the skew upwind differencing scheme of Raithby[17] is used, while for $1 \leq Pe_\Delta \leq 2$ the two schemes are weighted with a linear function of Pe_Δ. SHUDS was applied only to the solution of the momentum equations, whereas UWDS was used in all cases for the turbulent transport equations. As SHUDS leads to negative coefficients, there is a danger that, had it been used for the k and ε equations, negative values of these variables could have arisen during the solution. Even small negative values of k and ε have a catastrophic impact on the solution, and therefore must be avoided. It can be argued that UWDS can be legitimately used to solve for k and ε in those regions of the flow where the source terms in their equations are dominant and therefore the treatment of advection is unimportant. For other regions, the importance of the error in the present solution for these variables is unknown, and this factor requires attention in future studies.

Boundary conditions. The velocity boundary conditions at the solid walls in Figure 1 were zero velocity normal to the wall, and either zero tangential velocity for laminar flow or a specified shear stress based on wall functions[1] for turbulent flow. Fully developed conditions were used at the downstream boundary. At the inlet, the U-velocity profile was prescribed, and the cross-flow velocity, V, was set to zero. The boundary conditions on k and ε at the solid boundaries were treated in the standard[1] manner, and $\partial k/\partial x = \partial \varepsilon/\partial x = 0$ was used at the outlet. Further details relating to the inlet specification of velocities k and ε are described in later sections.

Solution. The equation sets arising from both the differencing schemes were solved in a similar manner. From best available estimates of the dependent variables, the coefficients in

the algebraic equations were calculated and the solution computed for the resulting linear set. The coefficients were then updated, a new solution found, and the process repeated until the following convergence criterion was satisfied:

$$(\Delta P_{ij}^{*})_{max}/[(P_{ij}^{*})_{max}-(P_{ij}^{*})_{min}] \leq 0{\cdot}0005$$

where the numerator represents the maximum change in pressure between solutions for consecutive sets of coefficients, and the denominator is the range in pressure throughout the solution domain. This criterion represents convergence close to the round-off limit on an IBM 4341 computer. When the criterion was met, the velocities obtained from the solution of the momentum equations satisfied mass conservation to the extent that the sum of the absolute values of the mass residuals, divided by the inlet mass flow rate, was generally less than 0·0002.

For a given set of coefficients, the equation sets were solved using the distorted transient method of Raithby and Schneider.[18] The SUMMIT (Sequential Update of Mass and Momentum for ImpliciT solution) method[3] maintained the strong implicit coupling between the mass and momentum equations necessary for rapid convergence.

Details related to the numerical model may be found in Hackman's thesis.[3]

RESULTS

Laminar flow

Numerical errors become pronounced when the artificial viscosity introduced by the differencing scheme overwhelms the correct effective viscosity of the flow. For this reason, high Reynolds number laminar flows are often more formidable to predict than turbulent flows; attention is therefore first directed to the prediction of laminar flow over a backward facing step. The inlet velocity profile was specified as parabolic along the broken line in Figure 1. The downstream boundary was located 20 step heights downstream of the step.

The predictions were made for $h/(h+H)=1/3$ in Figure 1, and for Reynolds numbers, based on h and the average in-flow velocity $\bar{U}$, of 73, 125, 191, and 229. These correspond to the experimental conditions of Denham and Pratrick.[19] Predictions were made using the UWDS and SHUDS schemes with both the Cartesian and curvilinear grids, at various levels of grid refinement (i.e. 4 separate predictions at each grid refinement level). The most sensitive feature of the flow appeared to be the reattachment length. This is plotted in Figure 3 for $Re=73$. For coarse grids, the 4 different prediction methods gave markedly different reattachment lengths, but for the finest grid (42×42) all predictions agreed to within 0·18 step heights. This is roughly the uncertainty in the interpolation necessary to locate the reattachment point; all the velocity profiles were virtually identical for the 42×42 grids. Figure 3 suggests that the Cartesian grid leads to smaller numerical errors, likely because the flow near separation remains more closely aligned with this grid which, in turn, leads to a lower numerical viscosity. The Cartesian-SHUDS scheme gave virtually identical results for all the grids used.

For the same geometry and inlet profile shape (parabolic), the velocity was increased to give a Reyhnolds number of 229. The change in the reattachment lengths for the 4 prediction methods with increasingly finer grids is shown in Figure 4. The Cartesian-SHUDS and curvilinear-SHUDS predictions agree for the fine grids to within 0·4 step heights, which is again roughly the uncertainty in the interpolation required to locate the reattachment point. The UWDS results in significantly different reattachment lengths, which approach the

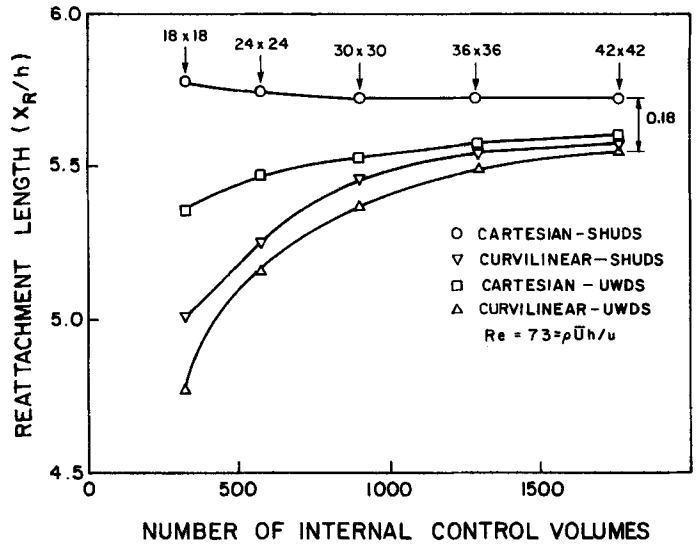

Figure 3. Predicted reattachment lengths for $Re = 73$ as a function of grid refinement. The grids shown include only control volumes within the computation domain

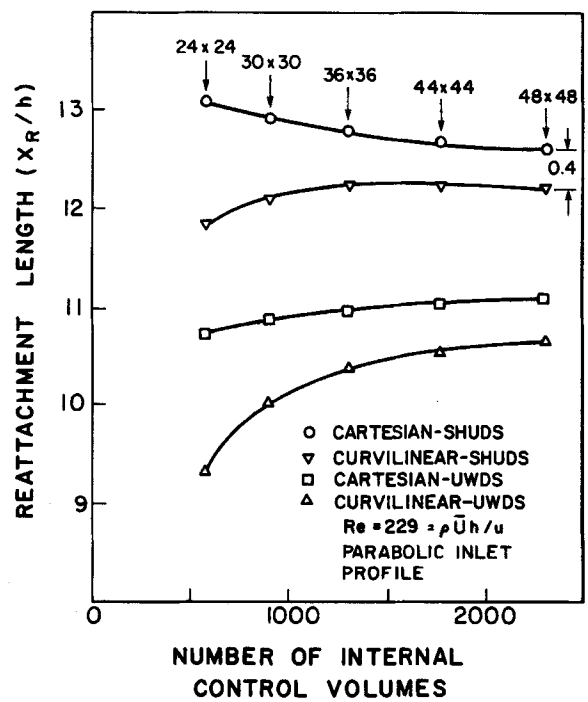

Figure 4. Predicted reattachment lengths for $Re = 229$ as a function of grid refinement. The grids shown include only control volumes within the computation domain

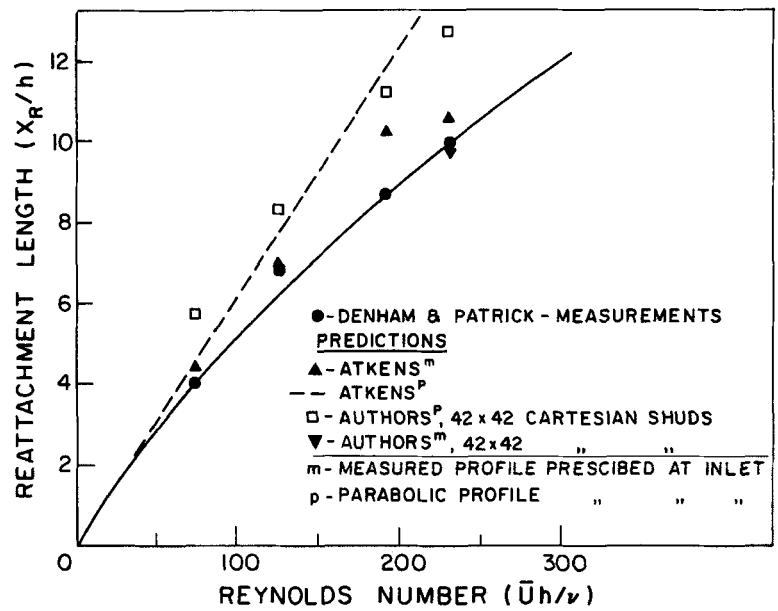

Figure 5. Comparison of the present predicted reattachment lengths with those of Patrick for a parabolic inlet profile (open symbols); solid symbols denote measurements, and predictions using the measured inlet profile

'correct' values from below. To obtain the same level of agreement as found for the lower Reynolds number (Figure 3), it is estimated that a grid of roughly 150×150 would be required if the UWDS were used. Calculations on such a grid were not economically feasible.

Figure 5 compares the predicted reattachment lengths for a parabolic inlet profile with those of Atkens *et al.*;[20] the maximum discrepancy in the predicted values of X_R/h is about 1·25. A prediction was also carried out using the 42×42 Cartesian mesh with the SHUDS scheme at $Re = 229$, but with the measured[21] inlet velocity profile in place of the parabolic profile. The predicted reattachment length, shown in Figure 5, was within 1 per cent of the observed value. The measured[21] and prescribed inlet velocities, and the predicted and measured velocities at various downstream stations, are shown in Figure 6. The agreement is entirely satisfactory.

The laminar flow study has underlined the problem of achieving accurate results using upstream weighted schemes. The SHUDS-scheme yields satisfactory results on a relatively coarse mesh.

Turbulent flow

As already mentioned, the backward facing step problem was chosen because of the availability of the accurate data of Kim.[2] The dimensions and fluid properties corresponding to Kim's experiment are tabulated in Figure 1. His data set included a comprehensive documentation of the inlet flow, as well as measurements of mean velocity, turbulent intensity and Reynolds stresses throughout the step region. The wall pressure was also determined.

Boundary conditions. The computation domain for this problem extended from the inflow boundary denoted by the dashed line in Figure 1, to 20 step heights downstream. The boundary conditions on the solid walls and downstream boundary were described earlier.

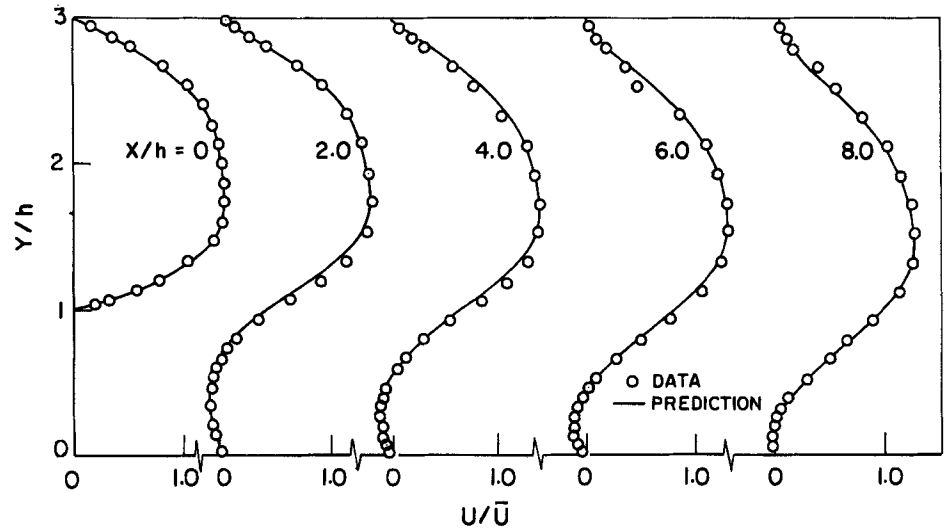

Figure 6. Comparison of the velocity measurements of Denham and Patrick[19] for $Re = 229$ with predictions. They used the measured velocity profile at the inlet boundary

The specification of the inlet profiles along the broken line in Figure 1 is particularly important and requires some explanation. Velocity profiles as well as some turbulence data were supplied by Kim at a distance $L_1 = 4h$ (see Figure 1) upstream of the step, and velocities were reported at the step. To prescribe the turbulence conditions at the step, the inlet channel between the measurement stations was treated as a section of a parallel plate duct with plate spacing H. The velocities measured at the station at distance L_1 upstream of the step, a turbulent kinetic energy estimated from the measured free stream turbulence intensity and a turbulent length scale equal to the channel width H, were all prescribed at the inlet. The flow in the parallel plate duct was then solved using a 50×50 grid, and the velocities, k and ε at a distance L_1 from the inlet of the duct (corresponding to the location of the broken line in Figure 1) were interpolated and used as the inlet condition for the step problem. A comparison of the predicted and measured velocities at the step indicated a maximum discrepancy between prediction and observation of 1 per cent.

Reattachment lengths. With these boundary conditions, predictions were again obtained for both Cartesian and curvilinear grids, for both the differencing schemes (UWDS and SHUDS), and for various levels of grid refinement. The reattachment length results are shown in Figure 7. The measured reattachment length of $7{\cdot}0h$ has an uncertainty of $\pm 0{\cdot}5h$, whereas the error from interpolation of the numerical results is about $\pm 0{\cdot}2h$. As in the laminar problem, reattachment lengths predicted by Cartesian-SHUDS and curvilinear-SHUDS were largest and least sensitive to grid refinement (to within the interpolation uncertainty), and the error bounds of these predictions and measurements overlap. Again, the UWDS results are less satisfactory.

Several investigators reported predictions for this problem at the Stanford Turbulent Flow Conference.[22] The predicted reattachment lengths obtained with the same k–ε model fell in the range $5{\cdot}2 < X_R/h < 6{\cdot}9$. The large difference between some of these values and the present predictions is apparently the result of solution error.

Velocity profiles. A comparison of velocity profiles indicated that results for the 36×36

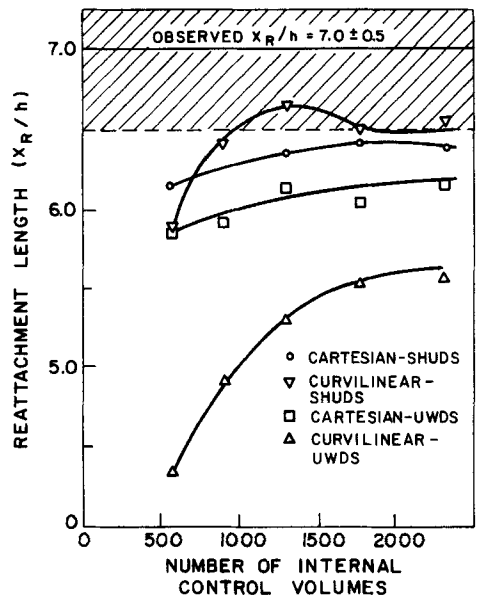

Figure 7. The effect of grid refinement on the predicted reattachment length for the 4 numerical schemes for turbulent flow. The measured value and the experimental uncertainty[19] are also shown

and 48×48 Cartesian-SHUDS prediction were indistinguishable. A very slight difference between these and the curvilinear-SHUDS predictions was attributed to the special treatment required in the application of boundary conditions for Cartesian-SHUDS at the singularities (lip and root of the step). The UWDS predictions showed a significant change with each grid refinement. The velocity profile comparisons therefore also suggested that the SHUDS results were, for practical purposes, grid independent.

In Figure 8, the 42×42 Cartesian-SHUDS predictions (indistinguishable from the 42×42

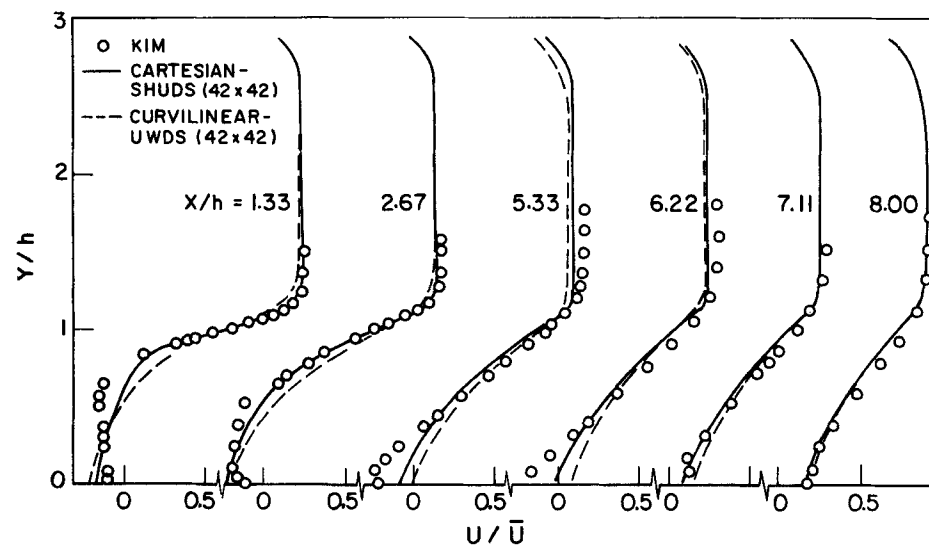

Figure 8. A comparison of predicted and measured velocities for the turbulent step flow problem of Kim[2] (see Figure 1)

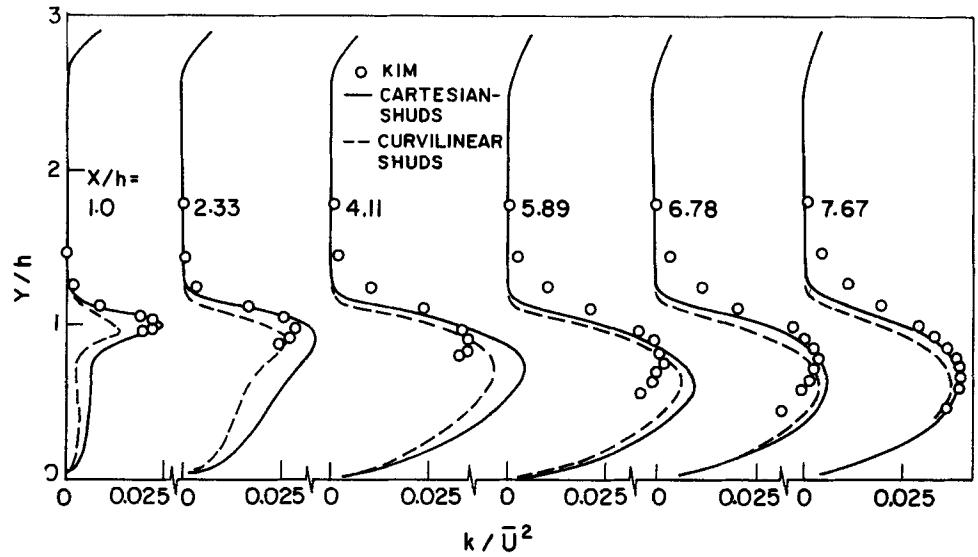

Figure 9. A comparison of predicted and 'measured' turbulent kinetic energy for Kim's[2] step flow problem (see Figure 1). Since the turbulence intensity in the Z direction was not measured, k was estimated by taking this to be the same as the measured intensity in the X direction

curvilinear-SHUDS predictions) are compared with Kim's measurements. Keeping in mind the relatively large experimental uncertainty within the recirculation zone, the predictions adequately reproduce the observations. The 42×42 curvilinear-UWDS predictions are also plotted in Figure 8. The upstream weighted scheme is seen to predict smaller velocity gradients, a result of the smearing caused by numerical diffusion.

Turbulent kinetic energy. The 42×42 Cartesian-SHUDS predictions of the kinetic energy at a few stations downstream of the step are plotted in Figure 9. These have been non-dimensionalized by $\bar{U}$. Since Kim reported only the u' and v' components of k, a kinetic energy was estimated by setting $w' = u'$; the resulting 'data' are plotted with the predictions in Figure 9. The predicted maximum values of k lie consistently higher than the data and the peak lies nearer the wall. Because of the method of estimating k, and because of experimental uncertainty of the measurements in the recirculation zone, it is not certain how much of the discrepancy results from the deficiency of the model. Certainly beyond the reattachment point the agreement near the peak is much improved.

The k–ε model does, however, appear to be deficient in the kinetic energy levels predicted near the edge of the potential core above the shear layer. The model maintains a sharp break in the kinetic energy distribution whereas the data suggest that k is significantly diffused into, or generated within, this region.

The 42×42 curvilinear-SHUDS predictions are also shown on the Figure. Although the velocities obtained using the two grids were virtually identical, the levels of k can be seen to be somewhat different for a 42×42 grid.

Turbulent stress. The predicted and measured turbulent stress is plotted in Figure 10. The model greatly overpredicts this quantity. Because the strain rates within the shear layer are roughly correct, this reflects the overprediction of either the turbulent kinetic energy or the turbulent length scale, or both.

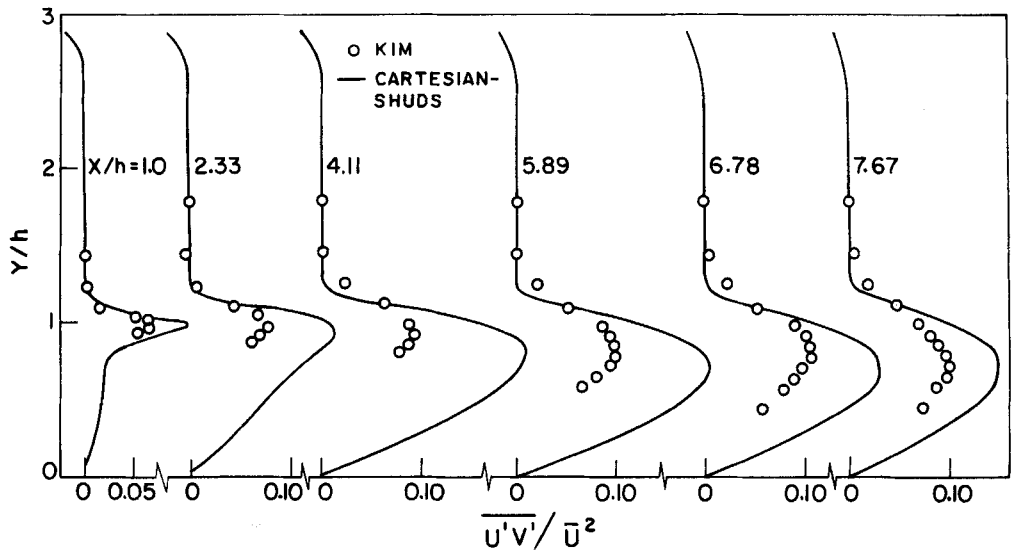

Figure 10. A comparison of the predicted and measured Reynolds stress for Kim's[2] step flow problem (see Figure 1)

Pressure recovery. Figure 11 shows the predicted pressure coefficient along the lower wall of the step, starting at the root, along with Kim's data. The overall pressure rise is well predicted, and the observed dip in the pressure before the recovery starts is reproduced. The predicted dip is initiated, however, too close to the step and the curve is displaced about one step height upstream of the data. The predictions of Kwon and Pletcher[9] are also reproduced on the graph. Their predictions agree with the data to roughly the same accuracy as the present predictions, but no dip was predicted and their overall pressure recovery was slightly below that observed.

Wall function application. Standard wall functions[1] were applied on the solid boundaries in the predictions already described. The wall generation of turbulent kinetic energy is not

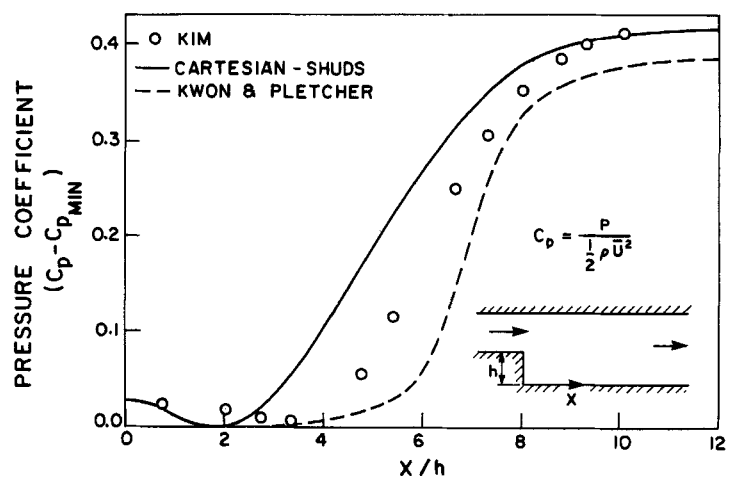

Figure 11. A comparison of the predicted and measured pressure recovery downstream of the step

well approximated by this treatment. To improve this estimate, the generation adjacent to boundaries was calculated from a three-equation approximation to the universal velocity profile, and the flow was recalculated using the 42×42 curvilinear-SHUDS method. This change caused the reattachment to increase from about 6·5 (see Figure 7) to 7·0, which is in better agreement with observation. However, only very minor changes resulted in other variables. The conclusion is that, for this problem, the accurate generation in the shear layer is much more important for the correct prediction of the recirculation zone than is the estimate of generation near the walls.

CONCLUSIONS

The present predictions of turbulent flow over a backward facing step are in significantly better agreement with measurement than are some previous predictions for the same problem using the same turbulence model. This change apparently results from the reduction of the error in solving the differential equations. It follows that to assess the adequacy of a turbulence model properly, extreme care is required to avoid confounding the error in the mathematical model with the solution error. The present study suggests that it is not feasible to use upstream differencing to obtain accurate solutions for recirculating turbulent flows. The skew hybrid upstream differencing scheme yielded virtually grid independent results with relatively coarse meshes.

ACKNOWLEDGEMENTS

This work was supported through operating grants from the Natural Sciences and Engineering Research Council of Canada. The authors wish to thank Mr. J. P. Van Doormaal for his important contributions to several phases of this work.

REFERENCES

1. B. E. Launder and D. B. Spalding, 'The numerical computation of turbulent flows', *Computer Methods in Applied Mechanics and Engineering*, **3**, 269–289 (1974).
2. J. J. Kim, 'Investigation of separation and reattachment of a turbulent shear layer: flow over a backward facing step', *Ph.D. Thesis*, Stanford University, 1978.
3. L. P. Hackman, 'A numerical study of the turbulent recirculating flow over a backward facing step using a two equation turbulence model', *Ph.D. Thesis*, University of Waterloo, Waterloo, Canada, 1982.
4. J. Militzer, W. B. Nicoll, and S. A. Alpay, 'Some observations on the numerical calculation of the recirculation region of twin parallel symmetric jet flow', *Proceedings of Turbulent Shear Flows I*, Springer-Verlag, 1977.
5. M. A. Leschziner and W. Rodi, 'Calculations of annular and twin parallel jets using various discretization schemes and turbulence-model variations', *J. of Fluids Engineering*, **103**, 352–360, (1981).
6. I. P. Castro, 'Numerical difficulties in the calculation of complex turbulent flows', *Proceedings of Turbulent Shear Flows I*, Springer-Verlag, 1977.
7. J. J. McGuirk, A. M. K. Taylor and J. H. Whitelaw, 'The assessment of numerical diffusion in upwind-difference calculations of turbulent recirculating flows', *Proceedings of Turbulent Shear Flows III*, University of California, Davis, 1981.
8. I. P. Castro, K. A. Cliffe and M. J. Norgett, 'Numerical predictions of the laminar flow over a normal flat plate' *Int. J. Num. Meth. Fluids*, **2**, 61–88 (1982).
9. O. K. Kwon and R. H. Pletcher, 'Prediction of the incompressible flow over a rearward facing step', *Technical Report ISU-ERI-Ames*-82019, Engineering Research Institute. Iowa State University, Ames, 1981.
10. F. Durst and A. K. Rastogi, 'Turbulent flow over two dimensional fences', a paper presented at the *Second Symposium on Turbulent Shear Flows*, Imperial College of Science and Technology, London, 1979.
11. B. E. Launder, 'Influence of numerics and computer variance in the computation of complex turbulent flows', *Proceedings of* 1981 *Stanford Conference on Complex Turbulent Flows*, Stanford University, Ca., March, 1982.
12. S. B. Pope, 'The calculation of turbulent recirculating flow in general orthogonal coordinates', *J. Comp. Phys.*, **26**, 197–217 (1978).
13. J. P. Van Doormaal, G. D. Raithby and A. B. Strong, 'Prediction of natural convection in non-rectangular enclosures using orthogonal curvilinear coordinates', *Numerical Heat Transfer*, **4**, 21–38 (1981).
14. S. V. Patankar, *Numerical Heat Transfer and Fluid Flow*, Hemisphere, 1980.

15. G. D. Raithby and K. E. Torrance, 'Upstream-weighted differencing schemes and their application to elliptic problems involving fluid flow', *Computers and Fluids*, **2,** 191–206 (1974).
16. S. V. Patankar and D. B. Spalding, 'A calculation procedure for heat, mass and momentum transfer in three dimensional parabolic flows', *Int. J. Heat and Mass Transfer*, **15,** 1787–1806 (1972).
17. G. D. Raithby, 'Skew upstream differencing schemes for problems involving fluid flow', *Computer Methods in Applied Mechanics and Engineering*, **9,** 153–164 (1976).
18. G. D. Raithby and G. E. Schneider, 'Numerical solution of problems in incompressible fluid flow: treatment of the velocity-pressure coupling', *Numerical Heat Transfer*, **2,** 417–440 (1979).
19. M. K. Denham, and M. A. Patrick, 'Laminar flow over a downstream facing step in a two dimensional flow channel', *Trans. Inst. Chem. Engrs.*, **52,** 361–367 (1974).
20. D. J. Atkens, S. J. Maskell and M. A. Patrick, 'Numerical prediction of separated flows', *Int. J. Num. Meth. Eng.*, **15,** 129–144 (1980).
21. M. A. Patrick, Personal communications, Dept. of Chem. Eng., University of Exeter, Exeter, U.K., 1982.
22. *Proceedings of the* 1981 *Stanford Conference on Complex Turbulent Flows*, Stanford University, Stanford, CA., September 1981.